
Article:
Al-Maliki, H., Meierhofer, A., Trummer, G. et al. (2 more authors) (2021) A new approach for modelling mild and severe wear in wheel-rail contacts. Wear, 476. 203761. ISSN 0043-1648

https://doi.org/10.1016/j.wear.2021.203761

Wear xxx (xxxx) xxx

Contents lists available at ScienceDirect

Wear

journal homepage: http://www.elsevier.com/locate/wear

A new approach for modelling mild and severe wear in wheel-rail contacts

H. Al-Maliki [a,*], A. Meierhofer [a], G. Trummer [a], R. Lewis [b], K. Six [a]

[a] Virtual Vehicle Research GmbH, Graz, Austria
[b] Department of Mechanical Engineering, The University of Sheffield, Sheffield, UK

ARTICLE INFO

Keywords:
Wheel-rail tribology
Wheel-rail contact
Wear modelling
Wear testing
Twin-disc

ABSTRACT

This paper presents a new approach for modelling the wear in wheel-rail contacts for a wide range of test and contact conditions (material pairing, load, creep, lubrication etc.) in the mild and severe wear regimes with one set of model coefficients. The approach is based on a detailed analysis of 56 Twin-Disc experiments in combination with existing knowledge from the literature. The model considers the thickness of the damaged layer caused by severe plastic shear deformations in the near-surface layer of wheel or rail and the maximum shear stress in the contact as the main influencing factors responsible for the observed wear behaviour. In this way, a much better prediction quality can be reached for varying test and contact conditions compared to the state of the art energy dissipation or sliding based approaches. The model includes a low number of model coefficients which are independent of test and contact conditions.

1. Introduction

Wear is one of several phenomena (rolling contact fatigue, martensite layers, etc.) causing damage in the wheel-rail interface. These damages result in high maintenance costs for both, wheels and rails, reduced vehicle availability and delays due to track closure for repairs. Understanding and predicting these kinds of damage are essential to reduce them on one hand and to handle them appropriately on the other. Wear is a complex, continuous and inevitable phenomenon influenced by numerous parameters. Wear modifies the shape of wheel and rail profiles which is generally not desirable as it creates dynamic effects. However, certain wear rates are thought to remove initiated fatigue micro-cracks at the surface which positively influences the service life of wheels and rails [1–3].

The work published in the literature reveals the great efforts to understand the wear behaviour in the wheel-rail contact. Researchers [4,5] showed that the development of the wear rate over the number of cycles frequently has a similar pattern as the coefficient of traction (CoT). Both are progressively rising in the first few thousand cycles until reaching the steady-state. CoT is regularly higher for dry contact than for contaminated contacts (water, grease [4], dry leaves and wet leaves [5], respectively) which is again true for the wear rate.

Several variables influence the wear rate: in addition to load, of course, wear is influenced by the type of rail [6,7] and wheel material [8,9]. Likewise, wear rate is changing with varying the contact conditions (dry or lubricated) [10–13], tangential forces, creep [14], operating speed [2,15], surface roughness [16,17], presence of 3rd body layers (iron oxides, etc.) [18] and developing material anisotropy [19–21]. Moreover, wear is related to several mechanisms occurring in the wheel-rail contact (abrasive wear, adhesive wear, delamination wear, tribo-chemical wear, fretting wear, surface fatigue wear and impact wear) [22].

The available experimental investigations illustrate the complexity of the wear phenomenon and the challenges that face its prediction. However, these investigations might not answer the most important question: what are the main physical dependencies behind wear in the wheel-rail contact?

Besides experiments, a lot of work can be found regarding wear modelling. Presently, two empirical wear modelling approaches are commonly used in scientific works. The first approach is the so-called sliding approach, it mainly depends on the sliding distance, load and material properties. This approach is primarily based on Archard's Adhesive model [23]. Several studies followed the sliding approach to model the wear in the wheel-rail contact [24,25].

The second approach is the so-called energy approach. This approach, as is evident from the name, assumes that the dissipated energy in the contact is mainly responsible for the development of wear. Several investigations have discussed the application of this approach [26–30]. Commonly, models belonging to the energy approach are correlating the wear rate with $T\gamma$ (product of tangential force and creep)

* Corresponding author.
E-mail address: Hayder.Al-Maliki@v2c2.at (H. Al-Maliki).

https://doi.org/10.1016/j.wear.2021.203761
Received 9 September 2020; Received in revised form 25 January 2021; Accepted 8 February 2021
Available online 22 March 2021

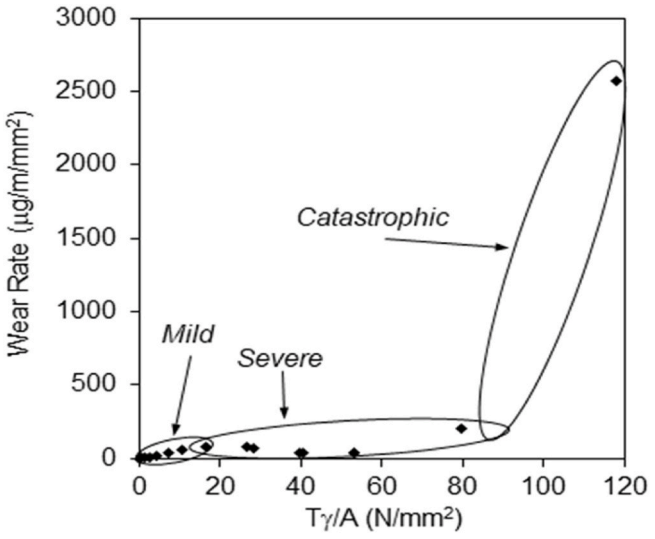

Fig. 1. Wear regime transitions in wheel-rail contact according to Tγ model [11].

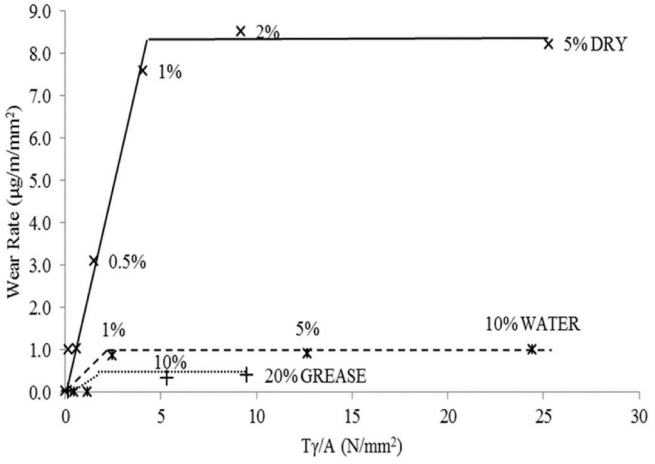

Fig. 2. Wear rates of R260 rail discs running against R8 wheel discs at 1500 MPa maximum contact pressure (contact conditions: dry, water-lubricated and grease-lubricated) according to Tγ model [11].

[31]. The Tγ model assumes that wear changes from mild to severe and to catastrophic with increasing Tγ/A (where A is the contact area), as shown in Fig. 1. Investigations with different contaminants show that wear rates change for given values of Tγ/A (at the same contact pressure) depending on the lubrication conditions (see Fig. 2). That means Tγ model needs new coefficients which need to be experimentally determined for each specific test (material pairing, load, creep, speed, etc.) and contact (dry, wet, grease lubricated, etc.) conditions which is also true for Archard's Adhesive model. These models may be useful for the conditions that the wear coefficients were generated at, however, they are unreliable to predict the wear rate for different test or contact conditions.

Extensive testing under varying test and contact conditions is needed for these models, causing high effort with large related costs. Thus, a more physical based wear model which implicitly accounts for the testing and contact conditions mentioned above would reduce the experimental effort and improve the prediction quality significantly. Such a prediction model for mild and severe wear regimes is presented in this work. The new model is based on the analysis of a big number of Twin-Disc experiments with different test and contact conditions from different sources (projects).

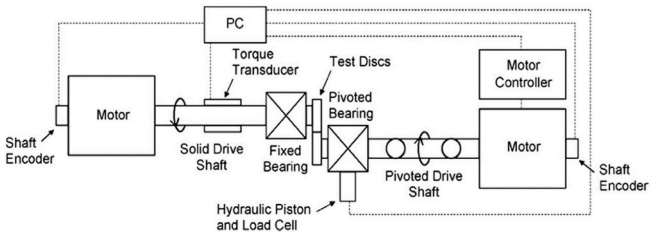

Fig. 3. Scheme showing SUROS Twin-Disc rig [11].

In Section 2, the wear testing methodology is presented and in Section 3, the wear testing results are presented and discussed. This is followed by the description, parameterisation and validation of the new wear model in Section 4. Final conclusions are drawn in Section 5.

2. Experimental methodology

2.1. Apparatus

Wear experiments were carried out using a Twin-Disc rig (rolling-sliding machine (SUROS)) at the University of Sheffield. A schematic showing the rig arrangements is depicted in Fig. 3. The development details, usages and limitations of the apparatus have been published earlier [32]. The test rig is built on a Colchester Mascot lathe with two independently driven (AC) motors at the tailstock end. Creep (cx) is produced by adjusting the speed of one of the motors. The rail disc acts as the driven or braking disc (slower) whereas the wheel disc performs as the driving disc (faster). The torque is monitored by a torque transducer on one of the rig shafts. The discs are pressed against each other using a hydraulic system. The data download frequency is 1 Hz to a PC which is also controlling the load and the creep of the test.

2.2. Specimens

The test specimens have a cylindrical form (disc) and are machined from wheel and rail sections, in particular, from the closest possible level to the wheel-tread and rail-head surfaces. The rail discs are always made of pearlitic rail steel grade R260, the material of wheel discs alters (pearlitic steel grade R8, R7 and R260). Wheel and rail discs have a diameter of 47 mm with a thickness (contact track width) of 10 mm. All samples are ground to a roughness (Ra) of about 1 μm to ensure comparable contact conditions initially.

2.3. Test configurations

56 test datasets from the SUROS Twin-Disc test rig at the University of Sheffield were used for this work. Only wear measurements within the ranges of mild and severe regimes according to the Tγ model were considered (Tγ/A of all experiments within 0–60 [N/mm^2]), to make sure that thermal effects do not influence the wear behaviour (see Fig. 1) [11,33]. These 56 measurements are divided into five groups (A, B, C, D and E) according to the source (project) from which they were taken. The R260 rail discs were running against wheel discs made of pearlitic wheel steel grade R8 in 46 tests. In 8 tests, the rail discs were running against wheel discs made of pearlitic wheel steel grade R7. In 2 tests, rail and wheel discs were manufactured from the same material (pearlitic rail steel grade R260). 50 tests were done at 1500 MPa maximum contact pressure (p_0) according to Hertzian theory and 6 tests were done at 900 MPa. The rotational speed is 400 rpm (≈1 m/s). However, 3 tests were performed at a speed of 220 rpm (≈0.5 m/s). All tests were carried out at constant creep without interruption except for the 2 tests with wheel and rail discs made of the same material. Most of the tests were run for at least 25 000 cycles to ensure the presence of a saturated plastic deformation layer and steady-state wear behaviour [11,34]. However, 2

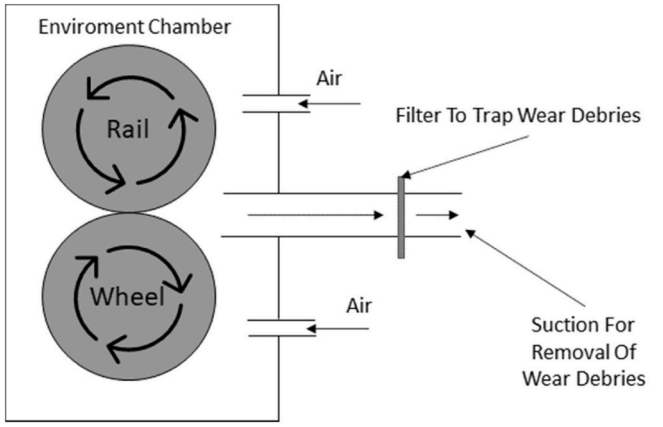

Fig. 4. Scheme presenting the technique of discs cooling and wear debris collection.

tests were run for 10 000 cycles at 0.01% creep and 3 tests were run for 15 000 cycles at 220 rpm.

The creep was varied from 0.01% to 20%. The lubrication conditions were dry, water and grease. Dripped water was supplied to the contact at a rate of 2 drops/second. The grease was manually and continuously supplied to the contact via a syringe. The mass loss due to wear was calculated as the difference between the original disc mass and the disc mass at the end of the run. The wear rate was measured in g/cycle. The discs were cleaned before and after the test in an acetone bath and left in ambient conditions until fully dry to ensure a precise mass loss calculation. Traction coefficient was calculated automatically from the online torque measurements. The ambient conditions were recorded to be in the range of 40%–50% for humidity and 20°C–25 °C for temperature.

As mentioned before, two special tests were prepared for the presented work with specific configurations as follows:

- The same material is used for wheel and rail discs (pearlitic rail steel grade R260).
- For the first test, $p_0 = 1500$ MPa and cx = 1.5%.
- For the second test, $p_0 = 900$ MPa and cx = 3%.
- The tests were run for 44 000 cycles and each test was stopped every 5000 cycles to measure the mass loss.
- The last 4000 cycles of each test were run at 0% creep (pure rolling) and the mass loss was measured every 500 cycles.
- The test was carried out in an environmentally controlled chamber and the air was circulated through it to avoid the rise in the temperature and to carry the wear debris to the filtering system, as shown in Fig. 4.
- The air is sucking from the outlet of the chamber where the filter is installed to trap wear debris for further investigations.

The aim behind switching the creep off for the last 4000 cycles is to get insight how the previously produced near-surface plastically deformed layer (damaged layer) behaves and wear mechanisms vary when no shear is being generated in the contact.

The discs were cut perpendicularly to the rotation axis to investigate the surface and subsurface metallography using optical microscopy (OM). The specimen was etched with Nital before the metallography inspection. The wear debris was analysed using scanning electron microscopy (SEM).

3. Experimental results and discussion

In order to develop a precise wear prediction model, it is important to determine the main factors which are influencing the wear rate in the contact. Therefore, the wear results are plotted over different variables.

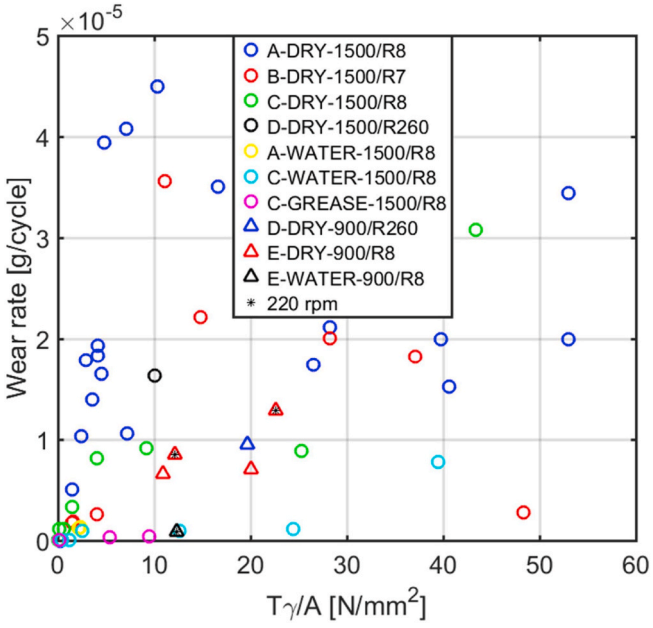

Fig. 5. Wear rate behaviour of R260 rail discs versus Tγ/A. (For interpretation of the references to colour in this figure legend, the reader is referred to the Web version of this article.)

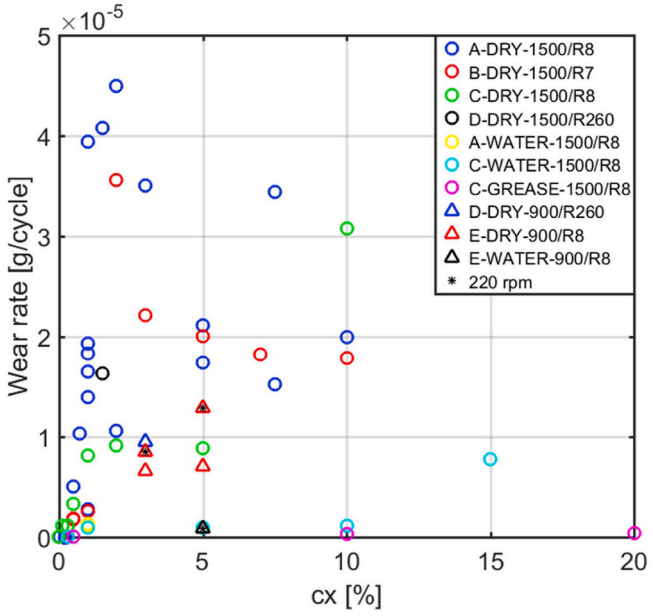

Fig. 6. Wear rate behaviour of R260 rail discs versus the creep. (For interpretation of the references to colour in this figure legend, the reader is referred to the Web version of this article.)

All available wear measurements from the SUROS machine of R260 rail discs are plotted over Tγ/A in Fig. 5, over the creep in Fig. 6, over the coefficient of traction in Fig. 7 and over maximum contact shear stress (τ) in Fig. 8. Due to the variety in the test and contact conditions, the results were divided into ten groups (see the legend of each plot). Each group indicates the source of the results, lubrication, maximum contact pressure and the material of the counter wheel disc, respectively. For example, the meaning of (A-DRY-1500/R8) in Fig. 5 as follows: "A" refers to the source of the results (project), "DRY" refers to the lubrication conditions (dry), "1500" refers to the maximum contact pressure in MPa and "R8" refers to the material of the wheel disc. "220 rpm"

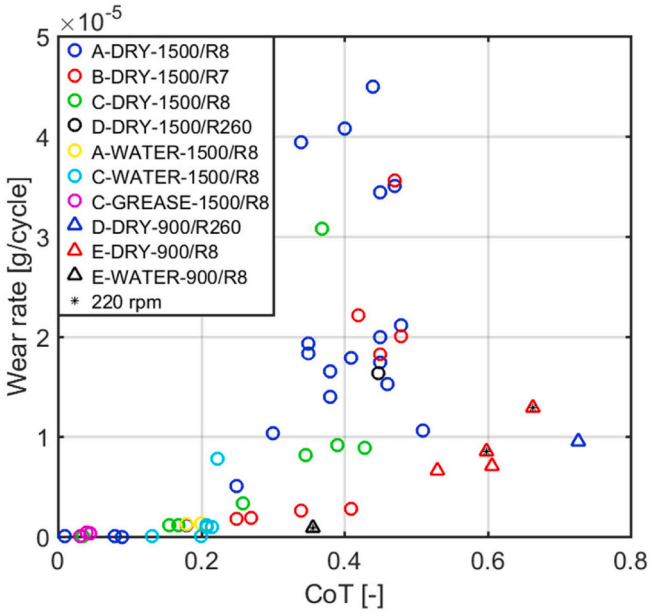

Fig. 7. Wear rate behaviour of R260 rail discs versus the coefficient of traction. (For interpretation of the references to colour in this figure legend, the reader is referred to the Web version of this article.)

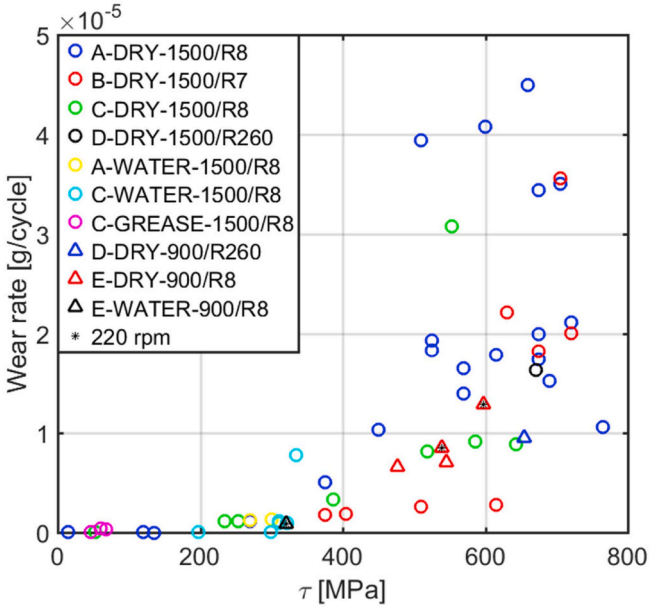

Fig. 8. Wear rate behaviour of R260 rail discs versus maximum contact shear stress. (For interpretation of the references to colour in this figure legend, the reader is referred to the Web version of this article.)

refers to the rolling speed.

When plotting all wear results over Tγ/A, no clear relationship can be seen (see Fig. 5) even though some individual groups such as (C-DRY-1500/R8) and (C-WATER-1500/R8) show similar behaviour as shown in Figs. 1 and 2.

Similar to Tγ/A, no clear correlation between wear rate and creep can be recognised (see Fig. 6).

The coefficient of traction in Fig. 7 represents the average value throughout the whole test run. In general, the wear rate shows rising behaviour with increasing CoT. The 900 MPa tests show a similar behaviour but on a lower level.

When plotting the wear results over the maximum shear stress in the contact, the differences between the 900 and the 1500 MPa results decrease, resulting in the best correlation with the wear rate even though there is still scattering visible (see Fig. 8). This correlation seems to be smooth at low τ, whereas more scattering is present with increasing the shear stress. The results of 1500 MPa are generally showing higher scattering than results of 900 MPa. Wear results fall on a single curve with altering the contact lubrication conditions. Furthermore, no significant influence of counter disc material and rolling speed on the wear rate is observed. A similar conclusion regarding the independence of wear on the material combinations and speed was noticed in the literature [35].

A few measurements show exceptionally high wear rates compared to the majority of measurements, in particular, at high shear stresses. This behaviour has been attributed to the following possible reasons:

- Differences in specimens' preparation (initial roughness).
- Machining tolerances not being met for the discs.
- Differences in the cleaning process before determining the mass loss (results from different sources).
- Slight differences in material properties, etc.

To summarise, the maximum shear stress in the contact shows the best correlation with the wear rate.

The better correlation with the maximum contact shear stress compared, for example, to the correlation with Tγ/A becomes even clearer when a moving average method is applied to the 1500 MPa data, see Fig. 9. Wear data for 900 MPa was not filtered due to the low number of data points and the low scattering. The legend gives information about the used filter parameters (window increment and window width), for example, the meaning of (Filtered-40-80-1500 MPa) in Fig. 9 b as follows: "Filtered" means data are filtered, "40" refers to the window increment (MPa), "80" refers to the window width (MPa) and "1500 MPa" refers to the maximum contact pressure. The filtered data show an obvious trend for wear over τ, whereas wear data still show no correlation with Tγ/A (Fig. 9 b and d). Filtering the data is providing additional evidence of wear dependency on maximum contact shear stress regardless of the testing and contact conditions. Therefore, this parameter needs to be considered in a reliable wear model for mild and severe wear regimes.

The presented work focuses on comparing the new wear modelling approach with the Tγ model. As mentioned in the introduction section, Archard's wear law considers the sliding distance as the main driving parameter responsible for wear (at constant load and material hardness). The sliding distance is directly proportional to the creep (cx) ($sliding\ distance/cycle = cx\ \pi\ d_{disc}$). Therefore, Fig. 6 can be considered as the relation between wear rate and sliding distance according to Archard's wear law (linear increase of wear rate with creep (sliding distance) would be expected), at least for every single group where the load and material combination were held constant. Considering the data in Fig. 6 at 1500 MPa, dry contact and running against R8 wheel discs (blue and green circles), no correlation can be recognised between wear rate and cx (sliding distance). The same is true for the rest of the experimental results.

Fig. 10 shows wear results from the special tests mentioned, where R260 rail discs were running against R260 wheel discs under dry contact conditions (p_0 = 1500 MPa, cx = 1.5% and p_0 = 900 MPa, cx = 3%). Wear rate increases in the first 10 000 cycles (run-in) then it becomes almost constant as it is described frequently. The wear is higher for the 1500 MPa test than for the 900 MPa test as expected.

From these experiments, additional information regarding relevant wear mechanisms can be extracted. After running the experiments for 40 000 cycles at a given creep, the creep was reduced to 0 (pure rolling). Instantly after switching the creep off, wear rates show a sharp increase dropping down after few hundreds of cycles. Interestingly, the wear rate does not go down to 0 as expected but seem to stabilise on a lower level

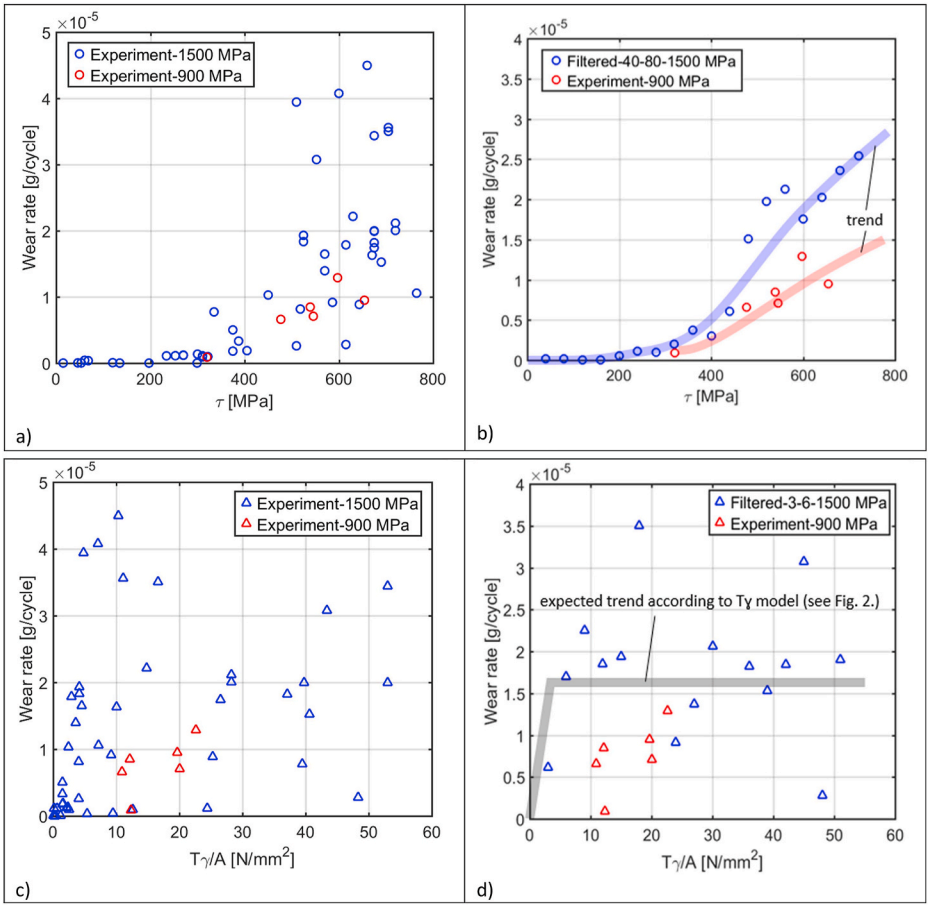

Fig. 9. Wear behaviour of R260 rail discs versus τ: a) raw, b) filtered and versus Tγ/A: c) raw, d) filtered. (For interpretation of the references to colour in this figure legend, the reader is referred to the Web version of this article.)

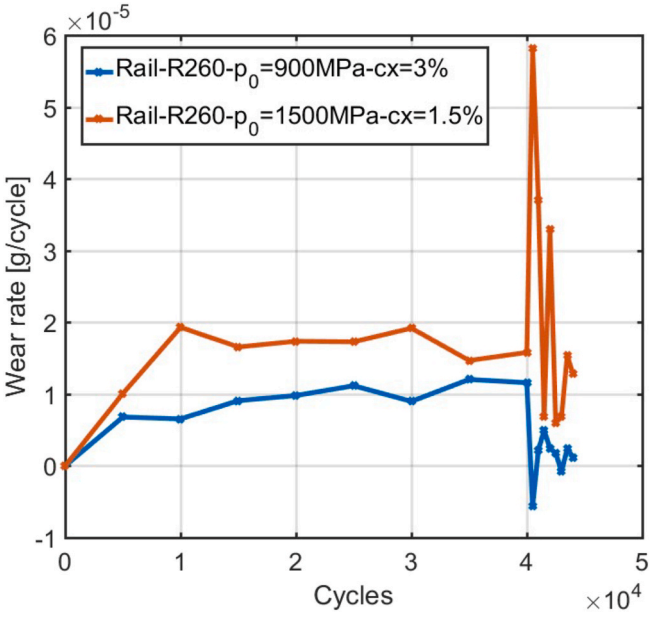

Fig. 10. Wear behaviour of R260 rail discs at p_0 = 900 MPa and 1500 MPa versus the number of cycles; test conditions: dry, counter disc material is R260, cx = 0% for 40k-44k cycles. (For interpretation of the references to colour in this figure legend, the reader is referred to the Web version of this article.)

compared to the situation before turning off the creep.

Empirical experience and reviewing the literature confirms the fact that under usual wheel-rail contact conditions, the material is mostly removed from wheel and rail surfaces according to the delamination theory [36–38]. Surface initiated micro-cracks grow along the aligned microstructure in the near-surface layer. This alignment is caused by the severe plastic shear deformation in this layer resulting in material anisotropy with respect to fatigue crack growth. This ends up in a flake-like structure near the surface oriented more or less parallel to the surface (see Fig. 11). This near-surface layer can be seen as a damaged material layer where flake-like wear debris gets continuously detached because of the contact loading situation.

This behaviour is confirmed by these special experiments. During the first 40 000 cycles, a damaged near-surface layer (with a flake-like structure) develops as a result of the combined cyclic normal and tangential contact loading. Flake-like wear debris gets detached from this damaged layer mainly due to the acting tangential shear stresses (see findings described before). After turning off the creep (at 40 000 cycles) the damage layer still exists and wear debris still gets detached but in this case because of other reasons (no shear stresses). Adhesion between the contacting surfaces pulling flakes from the surface when leaving the contact region (perpendicular to the surface) is expected to play a key role. It is expected that in the case of continuing such a test without creep (pure rolling), the damage layer gradually would get removed meaning that the wear rate would decrease continuously. This is an interesting topic for future research.

The tests with 1500 MPa maximum contact pressure show a thicker plastically deformed layer and a higher number of flakes at the surface than the 900 MPa tests, see Fig. 11. The R260 rail discs were running

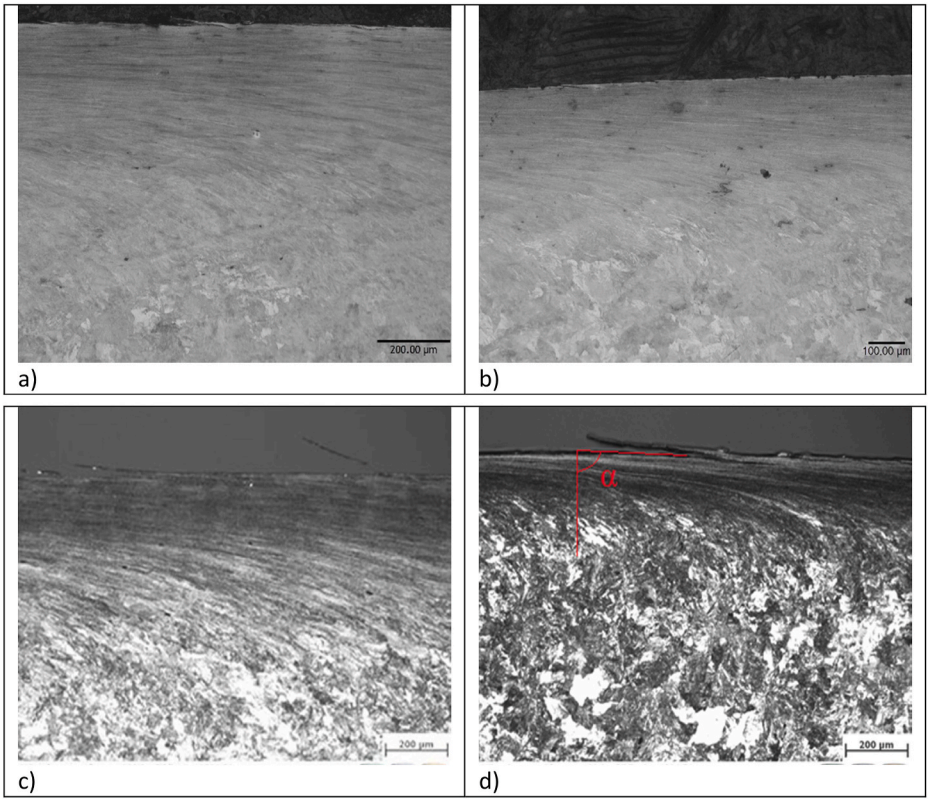

Fig. 11. Metallography (optical microscopy) of plastically deformed layer of R260 rail discs: a) R260/R260, $p_0 = 1500$ MPa, cx = 1.5%; b) R260/R260, $p_0 = 900$ MPa, cx = 3%; c) R260/R8, $p_0 = 1500$ MPa, cx = 1%; d) R260/R8, $p_0 = 900$ MPa, cx = 1%. (For interpretation of the references to colour in this figure legend, the reader is referred to the Web version of this article.)

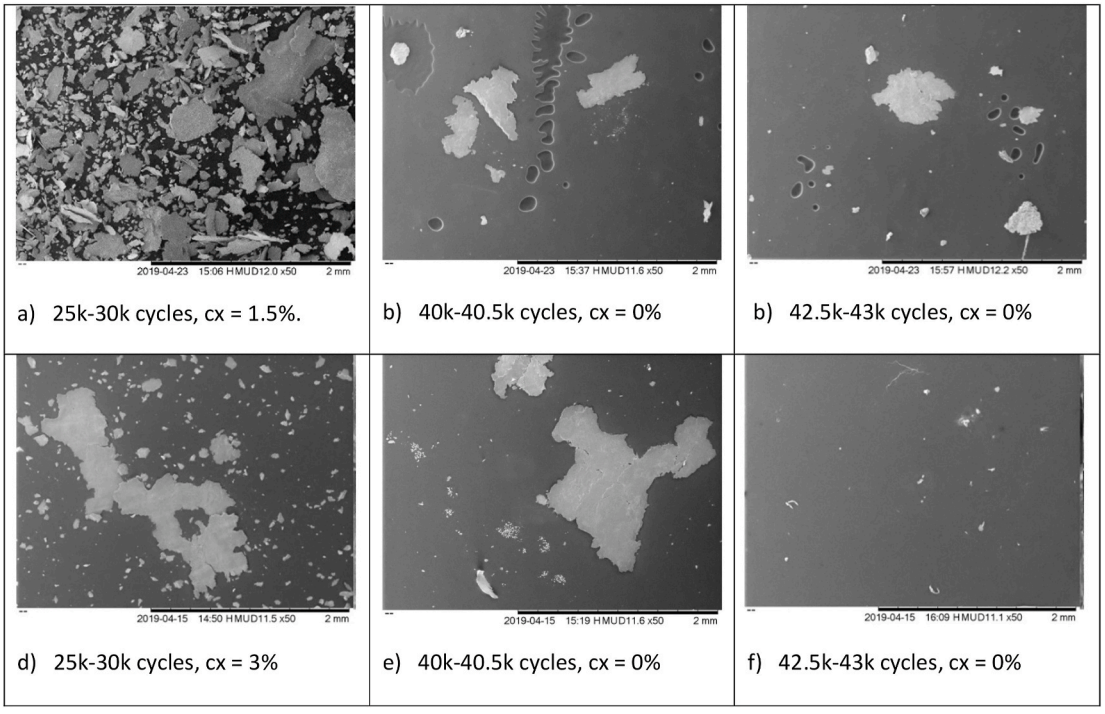

Fig. 12. SEM images of collected wear debris: $p_0 = 1500$ MPa in a), b), c) and $p_0 = 900$ MPa in d), e), f).

against R260 wheel discs (two tests of similar material for wheel and rail) in Fig. 11 a and b, while the R260 rail discs were running against R8 wheel discs (from another project) in Fig. 11 c and d.

The plastic deformation flow lines (visible due to the alignment of the microstructure with the shear plane) are inclined by an angle (α) measured from an axis perpendicular to the contact surface as shown in

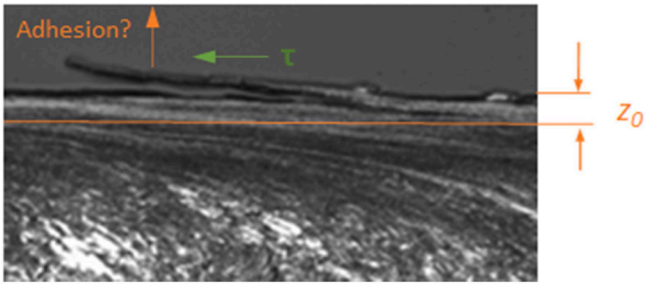

Fig. 13. Flake-like structure within the damaged layer (z_0) and the act of shear stresses and adhesion on the potential flake-like wear debris.

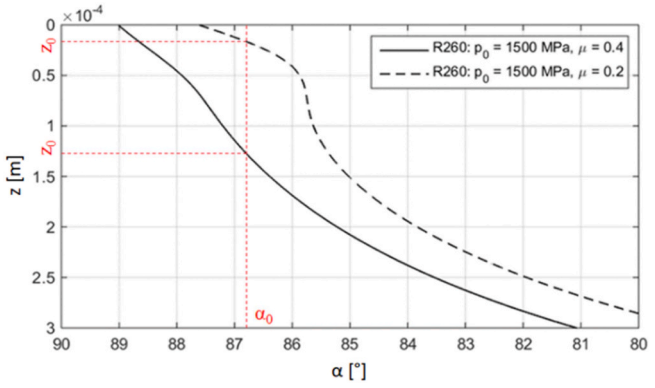

Fig. 14. Applying the plasticity model to predict the damage layer depth (z_0).

Fig. 11 d. This angle changes with depth, test conditions, contact conditions and material properties. This plastic shear strain angle (α) has its maximum at the surface and is dropping down with depth.

The SEM images of collected wear debris from the two special tests described above are shown in Fig. 12. Wear debris includes a mix of large and small flake-like particles in the wear steady-state when creep is applied (Fig. 12 a and d). The number of wear debris particles, in general, is higher for the 1500 MPa test compared to the 900 MPa test. At the beginning of the pure rolling (Fig. 12 b and e), the number of particles is dropping suddenly due to the absence of tangential stresses and the reduction of the cycles interval (500 cycles only). However, there are still flake-like wear particles visible. In the rest of the pure rolling run (Fig. 12 c and f), wear debris includes fine particles and again large flake-like debris for the 1500 MPa test. Altogether, the observed behaviour confirms that the highly deformed near-surface layer with its flake-like structure (damage layer) plays an important role regarding the wear behaviour of wheel and rail materials, even for pure rolling.

4. Wear modelling

4.1. Wear model

According to the experimental results presented and discussed before, the wear rate shows, on average, a much better correlation with τ than with Tγ/A (see Fig. 9).

Physically, the better correlation with τ makes sense under conditions with creep because of the flake-like structure of the damaged near-surface layer discussed above loaded by the contact shear stresses causing potential wear flakes to detach. Based on these observations, the following wear law is proposed:

$$Wear\ rate = k_1 z_0 + k_2 \tau^{k_3} \quad (1)$$

where wear rate is in [g/cycle], z_0 is in [m] and τ is in [MPa]. k_1, k_2 and k_3 are constant for a given material. Although this model still represents

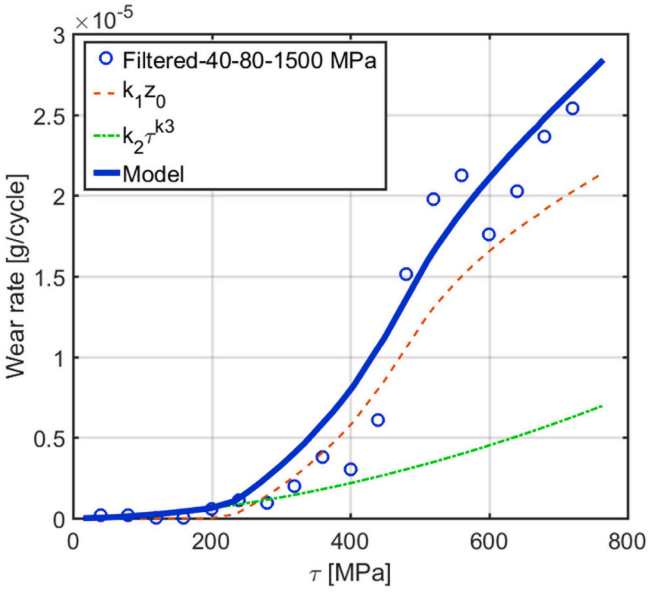

Fig. 15. Model parameterisation with wear data (R260 rail discs), p_0 = 1500 MPa. (For interpretation of the references to colour in this figure legend, the reader is referred to the Web version of this article.)

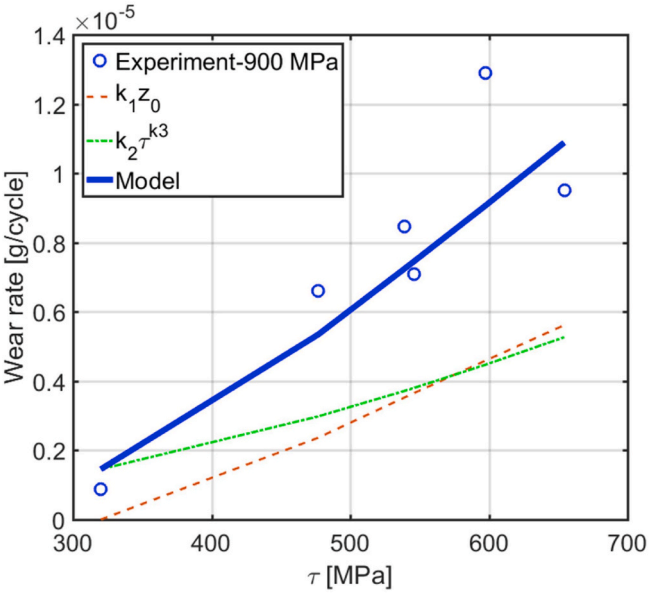

Fig. 16. Model parameterisation with wear data (R260 rail discs), p_0 = 900 MPa. (For interpretation of the references to colour in this figure legend, the reader is referred to the Web version of this article.)

an empirical approach, it accounts for the relevant physical effects observed in the tests. The model consists of two parts (see Fig. 13). The first part is the damage part ($k_1 z_0$) accounting for wear due to material damage in the highly plastically deformed near-surface layer. To calculate the depth of this damaged layer (z_0), the plasticity model [39, 40] is used in this work, however, it could also be determined by other researchers by finite element calculations using an elasto-plastic material law of the given material. The plasticity model predicts the angular shear strain (α) as a function of depth (z) depending on the normal and tangential contact stresses. z_0 is the value of z at a specific critical angular shear strain (α_0). α_0 represents the fourth model coefficient besides k_1, k_2, k_3 which is also assumed to be constant for a given material. The damage part of the wear law is active independent of shear

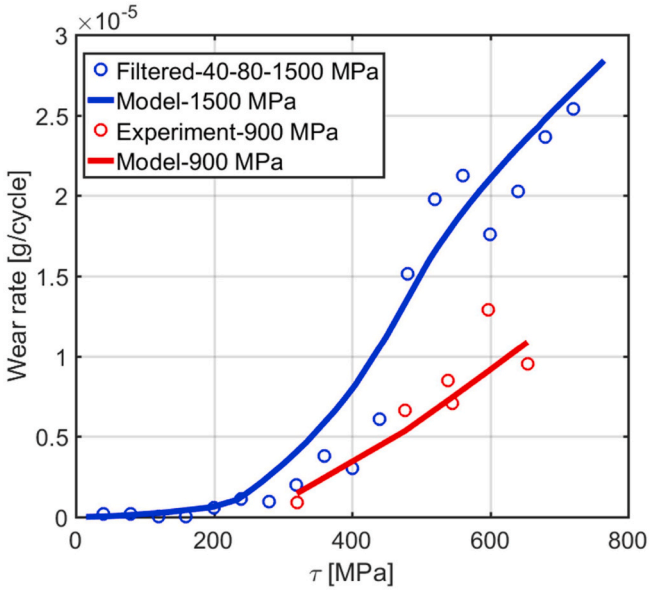

Fig. 17. Applying the new approach of wear modelling to predict the wear rate of R260 rail discs. (For interpretation of the references to colour in this figure legend, the reader is referred to the Web version of this article.)

Table 1
Wear model coefficients for R260 rail material (Twin-Disc).

k_1[g/m/cycle]	k_2[g/MPa^{k3}/cycle]	k_3[−]	α_0[°]
0.128	4.833×10^{-11}	1.739	86.807

stresses in the contact (adhesion could be the main mechanism when potential wear flakes leave the contact patch), although shear stresses might have been responsible for the development of the damaged layer due to the load history. Fig. 14 shows the process of estimating the thickness of the damaged layer (z_0) using the mentioned plasticity model for R260 rail material at 1500 MPa maximum contact pressure and two friction coefficients (assuming full sliding and steady-state conditions). Assuming α_0 being the critical angular shear strain, the model predicts two different thicknesses of the damaged layer (z_0).

The second part of the model represents the shear stress component ($k_2\tau^{k_3}$) where τ is the maximum shear stress in the contact (see Fig. 13).

The model coefficients k_1, k_2, k_3 and α_0 are determined by an optimisation procedure based on the squared errors between experimental and model results.

4.2. Wear model parameterisation

The wear model was parameterised considering all experimental data. The model is able to describe the average wear rate for R260 rail discs in the mild and severe regimes quantitatively. Fig. 15 and Fig. 16 show the model results together with data from the experiments for 1500 MPa and 900 MPa maximum contact pressure respectively. Additionally, the contributions from the damage and the shear stress parts of the wear model are plotted in these diagrams. It is important to highlight, that this is done with one set of model coefficients for R260 material regardless of test and contact conditions. The model nicely reproduces the differences between the 900 MPa and 1500 MPa maximum contact pressure results (see Fig. 17) because it includes the damage part ($k_1 z_0$) where z_0 increases with increasing contact pressure at a given maximum contact shear stress.

Table 1 summarises the wear model coefficients for R260 rail material to describe the wear rates observed in Twin-Disc experiments.

4.3. Wear model validation

As mentioned in the experimental results section, turning the creep off does not automatically mean that there is no material loss due to wear in the contact. If there is already a damaged layer on the surface because of load cycles with creep before turning off the creep, wear debris is still detached from the surface. This behaviour is considered in the proposed wear model by introducing the damage and the shear stress parts. In the case of creep, both model parts are active. After turning the creep off (pure rolling) the shear stress part is assumed to be inactive because of the absence of tangential stresses. The damage part in the case of pure rolling is the same as the damage part of the wear model immediately before switching the creep off. This is feasible because the related damaged layer has been developed by the normal stresses in combination with the tangential stresses before switching off the creep. Despite the complexity of this situation, the model is also able to predict the observed behaviour as shown in Fig. 18.

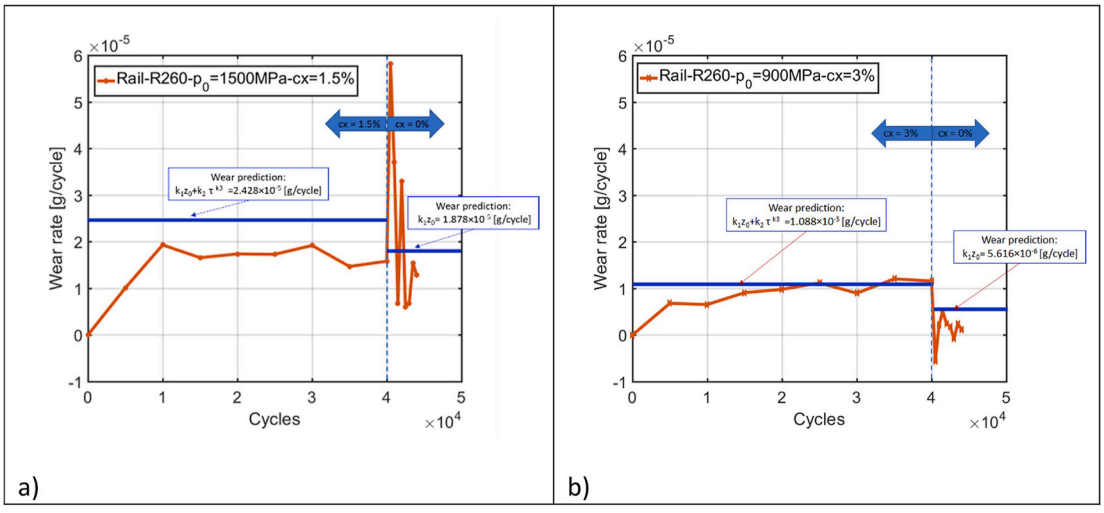

Fig. 18. Wear prediction for R260 rail disc running against R260 wheel disc: a) $p_0 = 1500$ MPa; b) $p_0 = 900$ MPa; For a) and b) cx = 0% after 40k cycles. (For interpretation of the references to colour in this figure legend, the reader is referred to the Web version of this article.)

5. Conclusion

- 56 experimental wear measurements from a Twin-Disc test rig (from different sources for different test and contact conditions) were collected and analysed.
- The data analysis showed a much better correlation between wear rate and maximum contact shear stress regardless of test and contact conditions compared to the correlation with $T\gamma/A$.
- Two special experiments were performed by using the same material (R260) for wheel and rail discs where the creep was turned off after 40 000 cycles to get additional information regarding the relevant wear mechanism in the wheel-rail contact.
- The transition to pure rolling after running at a given creep showed a drop of the wear rate (after initial fluctuation) to a lower level but not to 0 as it was expected.
- The results of these special experiments together with metallographic and SEM post-testing investigations confirmed that wear in wheel-rail contacts is driven by the delamination theory where a flake-like structure of the near-surface layer as a result of severe plastic shear deformation plays a key role (damage layer).
- Based on the experimental findings, a new model for mild and severe wear in wheel-rail contacts has been developed.
- The model consists of two parts, a damage part dependent on the depth of the damaged layer and shear stress part accounting for the influence of the maximum contact shear stress.
- The model is able to predict the average wear rate quantitatively for Twin-Disk test conditions.
- The model is also able to predict the behaviour for the complex case when the creep is turned off after initial cycles with creep.
- The new approach presents a radically new, physical-based and accurate method to predict the mild and severe wear rates observed in Twin-Disc experiments under very different test and contact conditions with one set of model coefficients for a given material.

Future work includes the extension of the developed model to consider the catastrophic wear regime. Furthermore, the applicability of the new model to full-scale conditions will be investigated based on experimental results from full-scale tests.

Declaration of competing interest

The authors declare that they have no known competing financial interests or personal relationships that could have appeared to influence the work reported in this paper.

Acknowledgements

The publication was written at Virtual Vehicle Research GmbH in Graz, Austria. The authors would like to acknowledge the financial support within the COMET K2 Competence Centers for Excellent Technologies from the Austrian Federal Ministry for Climate Action (BMK), the Austrian Federal Ministry for Digital and Economic Affairs (BMDW), the Province of Styria (Dept. 12) and the Styrian Business Promotion Agency (SFG). The Austrian Research Promotion Agency (FFG) has been authorised for the programme management. They would furthermore like to express their thanks to their supporting industrial and scientific project partners, namely Siemens Mobility Austria GmbH, voestalpine Rail Technology GmbH and the University of Sheffield.

References

[1] A. Kapoor, D.I. Fletcher, F.J. Franklin, The role of wear in enhancing rail life, Tribol. Res. Des. Eng. Syst. (2003) 331–340, https://doi.org/10.1016/S0167-8922(03)80146-3.
[2] C.G. He, J. Guo, Q.Y. Liu, W.J. Wang, Experimental investigation on the effect of operating speeds on wear and rolling contact fatigue damage of wheel materials, Wear 364–365 (2016) 257–269, https://doi.org/10.1016/j.wear.2016.08.006.
[3] G. Donzella, M. Faccoli, A. Mazzù, C. Petrogalli, R. Roberti, Progressive damage assessment in the near-surface layer of railway wheel-rail couple under cyclic contact, Wear 271 (2011) 408–416, https://doi.org/10.1016/j.wear.2010.10.042.
[4] C.T. Foo, B. Omar, A.S. Jalil, A review on recent wheel/rail interface friction management, J. Phys. Conf. Ser. 1049 (2018), 012009, https://doi.org/10.1088/1742-6596/1049/1/012009.
[5] E.A. Gallardo-Hernandez, R. Lewis, Twin disc assessment of wheel/rail adhesion, Wear 265 (2008) 1309–1316, https://doi.org/10.1016/j.wear.2008.03.020.
[6] J. Liu, W. Jiang, S. Chen, Q. Liu, Effects of rail materials and axle loads on the wear behavior of wheel/rail steels, Adv. Mech. Eng. 8 (2016), https://doi.org/10.1177/1687814016657254, 168781401665725.
[7] R. Lewis, W.J. Wang, M. Burstow, S.R. Lewis, Investigation of the influence of rail hardness on the wear of rail and wheel materials under dry conditions, in: 11th Int. Conf. Contact Mech. Wear Rail/Wheel Syst. (CM2018), 2018, pp. 1–8, https://doi.org/10.4203/ccp.110.151. Delft, Netherlands, Sept. 24-27, 2018 Investig.
[8] W. Wang, W. Jiang, H. Wang, Q. Liu, M. Zhu, X. Jin, Experimental study on the wear and damage behavior of different wheel/rail materials, Proc. Inst. Mech. Eng. - Part F J. Rail Rapid Transit 230 (2016) 3–14, https://doi.org/10.1177/0954409714524566.
[9] W.T. Zhu, L.C. Guo, L.B. Shi, Z.B. Cai, Q.L. Li, Q.Y. Liu, W.J. Wang, Wear and damage transitions of two kinds of wheel materials in the rolling-sliding contact, Wear 398–399 (2018) 79–89, https://doi.org/10.1016/j.wear.2017.11.023.
[10] L.C. Guo, W.T. Zhu, L.B. Shi, Q.Y. Liu, Z.B. Cai, W.J. Wang, Study on wear transition mechanism and wear map of CL60 wheel material under dry and wet conditions, Wear 426–427 (2019) 1771–1780, https://doi.org/10.1016/j.wear.2018.12.049.
[11] C. Hardwick, R. Lewis, D.T. Eadie, Wheel and rail wear—understanding the effects of water and grease, Wear 314 (2014) 198–204, https://doi.org/10.1016/j.wear.2013.11.020.
[12] R. Lewis, R.S. Dwyer-Joyce, Wear mechanisms and transitions in railway wheel steels, Proc. Inst. Mech. Eng. Part J J. Eng. Tribol. 218 (2004) 467–478, https://doi.org/10.1243/1350650042794815.
[13] A. Meierhofer, G. Trummer, C. Bernsteiner, K. Six, Vehicle tests showing how the weather in autumn influences the wheel–rail traction characteristics, Proc. Inst. Mech. Eng. - Part F J. Rail Rapid Transit 234 (2019) 426–435, https://doi.org/10.1177/0954409719863643.
[14] C.G. He, Y.B. Huang, L. Ma, J. Guo, W.J. Wang, Q.Y. Liu, M.H. Zhu, Experimental investigation on the effect of tangential force on wear and rolling contact fatigue behaviors of wheel material, Tribol. Int. 92 (2015) 307–316, https://doi.org/10.1016/j.triboint.2015.07.012.
[15] H.H. Ding, Z.K. Fu, W.J. Wang, J. Guo, Q.Y. Liu, M.H. Zhu, Investigation on the effect of rotational speed on rolling wear and damage behaviors of wheel/rail materials, Wear 330–331 (2015) 563–570, https://doi.org/10.1016/j.wear.2014.12.043.
[16] A. Khalladi, K. Elleuch, Effect of surface topography with different groove angles on tribological behavior of the wheel/rail contact using alternative machine, Friction 4 (2016) 238–248, https://doi.org/10.1007/s40544-016-0121-y.
[17] Y. Lyu, E. Bergseth, U. Olofsson, A. Lindgren, M. Höjer, On the relationships among wheel–rail surface topography, interface noise and tribological transitions, Wear 338–339 (2015) 36–46, https://doi.org/10.1016/j.wear.2015.05.014.
[18] T. Nakahara, K.-S. Baek, H. Chen, M. Ishida, Relationship between surface oxide layer and transient traction characteristics for two steel rollers under unlubricated and water lubricated conditions, Wear 271 (2011) 25–31, https://doi.org/10.1016/j.wear.2010.10.030.
[19] M. Masoumi, A. Sinatora, H. Goldenstein, Role of microstructure and crystallographic orientation in fatigue crack failure analysis of a heavy haul railway rail, Eng. Fail. Anal. 96 (2019) 320–329, https://doi.org/10.1016/j.engfailanal.2018.10.022.
[20] A. Ekberg, Anisotropy and rolling contact fatigue of railway wheels, Int. J. Fatig. 23 (2001) 29–43, https://doi.org/10.1016/S0142-1123(00)00070-0.
[21] B. Dylewski, M. Risbet, S. Bouvier, The tridimensional gradient of microstructure in worn rails – experimental characterization of plastic deformation accumulated by RCF, Wear 392–393 (2017) 50–59, https://doi.org/10.1016/j.wear.2017.09.001.
[22] H. Soleimani, M. Moavenian, Tribological aspects of wheel–rail contact: a review of wear mechanisms and effective factors on rolling contact fatigue, Urban Rail Transit 3 (2017) 227–237, https://doi.org/10.1007/s40864-017-0072-2.
[23] J.F. Archard, Contact and rubbing of flat surfaces, J. Appl. Phys. 24 (1953) 981–988, https://doi.org/10.1063/1.1721448.
[24] A. Ramalho, Wear modelling in rail–wheel contact, Wear 330–331 (2015) 524–532, https://doi.org/10.1016/j.wear.2015.01.067.
[25] R. Enblom, M. Berg, Simulation of railway wheel profile development due to wear—influence of disc braking and contact environment, Wear 258 (2005) 1055–1063, https://doi.org/10.1016/j.wear.2004.03.055.
[26] R. Lewis, R. Dwyer-Joyce, N. Tassini, N. Kuka, C. Ariaudo, X. Quost, A numerical model of twin disc test arrangement for the evaluation of railway wheel wear prediction methods, Wear 268 (2009) 660–667, https://doi.org/10.1016/j.wear.2009.11.003.
[27] A. Rovira, A. Roda, M.B. Marshall, H. Brunskill, R. Lewis, Experimental and numerical modelling of wheel–rail contact and wear, Wear 271 (2011) 911–924, https://doi.org/10.1016/j.wear.2011.03.024.
[28] T.G. Pearce, N.D. Sherratt, Prediction of wheel profile wear, Wear 144 (1991) 343–351, https://doi.org/10.1016/0043-1648(91)90025-.
[29] N. Zobory, Prediction of wheel/rail profile wear, Veh. Syst. Dyn. 28 (1997) 221–259, https://doi.org/10.1080/00423119708969355.

[30] H. Krause, G. Poll, Wear of wheel-rail surfaces, Wear 113 (1986) 103–122, https://doi.org/10.1016/0043-1648(86)90060-8.
[31] R. Lewis, F. Braghin, A. Ward, S. Bruni, R.S. Dwyer-Joyce, K.B. Knani, P. Bologna, Integrating dynamics and wear modelling to predict railway wheel profile evolution, in: 6th Int. Conf. Contact Mech. Wear Rail/Wheel Syst. C. CHARMEC, Gothenbg., 2003. https://pdfs.semanticscholar.org/510d/b1b239eceac9e90a45d34e949f39bd3b8d59.pdf.
[32] D.I. Fletcher, J.H. Beynon, Development of a machine for closely controlled rolling contact fatigue and wear testing, J. Test. Eval. 28 (2000) 267–275, https://doi.org/10.1520/JTE12104J.
[33] W.J. Wang, R. Lewis, B. Yang, L.C. Guo, Q.Y. Liu, M.H. Zhu, Wear and damage transitions of wheel and rail materials under various contact conditions, Wear 362–363 (2016) 146–152, https://doi.org/10.1016/j.wear.2016.05.021.
[34] P. Christoforou, D.I. Fletcher, R. Lewis, Benchmarking of premium rail material wear, Wear 436–437 (2019) 202990, https://doi.org/10.1016/j.wear.2019.202990.
[35] P.J. Bolton, P. Clayton, Rolling—sliding wear damage in rail and tyre steels, Wear 93 (1984) 145–165, https://doi.org/10.1016/0043-1648(84)90066-8.
[36] G. Trummer, C. Marte, P. Dietmaier, C. Sommitsch, K. Six, Modeling surface rolling contact fatigue crack initiation taking severe plastic shear deformation into account, Wear 352–353 (2016) 136–145, https://doi.org/10.1016/j.wear.2016.02.008.
[37] W.R. Tyfour, J.H. Beynon, The effect of rolling direction reversal on the wear rate and wear mechanism of pearlitic rail steel, Tribol. Int. 27 (1994) 401–412, https://doi.org/10.1016/0301-679X(94)90017-5.
[38] N.P. Suh, An overview of the delamination theory of wear, Wear 44 (1977) 1–16, https://doi.org/10.1016/0043-1648(77)90081-3.
[39] G. Trummer, K. Six, C. Marte, A. Meierhofer, C. Sommitsch, Automated measurement of near-surface plastic shear strain, in: J. Pombo (Ed.), Proc. Second Int. Conf. Railw. Technol. Res. Dev. Maint., Civil-Comp Press, Stirlingshire, United Kingdom, 2014, https://doi.org/10.4203/ccp.104.104.
[40] G. Trummer, K. Six, C. Marte, P. Dietmaier, C. Sommitsch, An approximate model to predict near-surface ratcheting of rails under high traction coefficients, Wear 314 (2014) 28–35, https://doi.org/10.1016/j.wear.2013.11.019.